Title
Regulation of Brain Primary Cilia Length by MCH Signaling: Evidence from Pharmacological, Genetic, Optogenetic, and Chemogenic Manipulations

Journal
Molecular Neurobiology, 59(1)

ISSN
0893-7648

Authors
Alhassen, Wedad
Kobayashi, Yuki
Su, Jessica
et al.

Publication Date
2022

DOI
10.1007/s12035-021-02511-w

Peer reviewed

HHS Public Access

Author manuscript

Mol Neurobiol. Author manuscript; available in PMC 2022 May 09.

Published in final edited form as:

Mol Neurobiol. 2022 January ; 59(1): 245–265. doi:10.1007/s12035-021-02511-w.

Regulation of Brain Primary Cilia Length by MCH Signaling: Evidence from Pharmacological, Genetic, Optogenetic, and Chemogenic Manipulations

Wedad Alhassen[1], **Yuki Kobayashi**[2], **Jessica Su**[1], **Brianna Robbins**[1], **Henry Nguyen**[1], **Thant Myint**[1], **Micah Yu**[1], **Surya M. Nauli**[3], **Yumiko Saito**[2], **Amal Alachkar**[1,4]

[1]Departments of Pharmaceutical Sciences, School of Pharmacy, University of California, Irvine, CA 92697, USA

[2]Graduate School of Integrated Sciences for Life, Hiroshima University, 1-7-1 Kagamiyama, Higashi-Hiroshima, Hiroshima 739-8521, Japan

[3]Department of Biomedical and Pharmaceutical Sciences, School of Pharmacy, Chapman University, Health Science Campus, Chapman University, Irvine, CA 92618, USA

[4]Institute for Genomics and Bioinformatics, School of Information and Computer Sciences, University of California, Irvine, CA 92697, USA

Abstract

The melanin-concentrating hormone (MCH) system is involved in numerous functions, including energy homeostasis, food intake, sleep, stress, mood, aggression, reward, maternal behavior, social behavior, and cognition. In rodents, MCH acts on MCHR1, a G protein-coupled receptor, which is widely expressed in the brain and abundantly localized to neuronal primary cilia. Cilia act as cells' antennas and play crucial roles in cell signaling to detect and transduce external stimuli to regulate cell differentiation and migration. Cilia are highly dynamic in terms of their length and morphology; however, it is not known if cilia length is causally regulated by MCH system activation in vivo. In the current work, we examined the effects of activation and inactivation of MCH system on cilia lengths by using different experimental models and

Amal Alachkar, aalachka@uci.edu.

Author Contribution AA designed the experiments and wrote the manuscript; WA and JS conducted the in vivo experiments; YK conducted the ex vivo experiments; BR, HN, TM, and SA contributed to data analysis. SN and YS contributed to the experimental design and manuscript writing.

Supplementary Information The online version contains supplementary material available at https://doi.org/10.1007/s12035-021-02511-w.

Ethics Approval All experimental procedures were reviewed and approved by the Hiroshima University Animal Care Committee and met the Japanese Experimental Animal Research Association standards, as defined in the Guidelines for Animal Experiments (1987), and the Institutional Animal Care and Use Committee of the University of California, Irvine. All experiments were performed in compliance with national and institutional guidelines for the care and use of laboratory animals.

Competing Interests The authors declare no competing interests.

Research Resource Identifiers (RRID) AAV5-EF1a-DIO-ChR2-T159c-eYFP # 35509-AAV5: Addgene_35509.
AAV8-hSyn-DIO-hM3D(Gq)-mCherry #44361-AAV8:Addgene_44361). Histo VT One: Nacalai Tesque, Kyoto, Japan.
Alexa Fluor 488-conjugated donkey anti-rabbit IgG: Thermo Fisher Scientific, Rockford, IL, USA Alexa Fluor 546-conjugated donkey anti-goat IgG: Thermo Fisher Scientific.
Anti-MCH antibody: courtesy of W. Vale, Salk Institute, La Jolla, CA, USA.
Anti-c-Fos antibody: Invitrogen, USA.
Goat anti-human MCHR1: C-17, sc-5534; Santa Cruz Biotechnology, USA.

methodologies, including organotypic brain slice cultures from rat prefrontal cortex (PFC) and caudate–putamen (CPu), in vivo pharmacological (MCHR1 agonist and antagonist GW803430), germline and conditional genetic deletion of MCHR1 and MCH, optogenetic, and chemogenetic (designer receptors exclusively activated by designer drugs (DREADD)) approaches. We found that stimulation of MCH system either directly through MCHR1 activation or indirectly through optogenetic and chemogenetic-mediated excitation of MCH-neuron, caused cilia shortening, detected by the quantification of the presence of ADCY3 protein, a known primary cilia marker. In contrast, inactivation of MCH signaling through pharmacological MCHR1 blockade or through genetic manipulations — germline deletion of MCHR1 and conditional ablation of MCH neurons — induced cilia lengthening. Our study is the first to uncover the causal effects of the MCH system in the regulation of the length of brain neuronal primary cilia. These findings place MCH system at a unique position in the ciliary signaling in physiological and pathological conditions and implicate MCHR1 present at primary cilia as a potential therapeutic target for the treatment of pathological conditions characterized by impaired primary cilia function associated with the modification of its length.

Keywords

Cilia; Melanin-concentrating hormone; Signaling; Brain; Activation; Inactivation

Introduction

Melanin-concentrating hormone (MCH), a 19 amino acid hypothalamic neuropeptide, is involved in numerous functions, including food intake, energy homeostasis, arousal, sleep, learning and memory, cognition, emotions, and maternal behavior [4, 13, 14, 18, 22, 23, 34, 35, 60, 63, 64, 82]. Dysregulation of the MCH system has been linked to psychiatric and neurological disorders such as depression anxiety and, most recently, schizophrenia and Alzheimer's disease [58, 83].

MCH exerts its actions through activating the G protein-coupled receptor (GPCR) MCHR1 that is widely distributed throughout the brain [68, 69]. MCHR1 couples to Gi/o and Gq, resulting in the activation of signaling pathways, including Ca^{2+} mobilization, ERK phosphorylation, and inhibition of cyclic AMP generation. MCHR1 receptors are abundantly found in neuronal primary cilia [8, 26, 43], protrusions from the cell bodies of neurons that act as antennas for cells. Cilia are responsible for signaling functions, including detecting and transducing external stimuli crucial for the maintaining homeostasis (see [10, 85], for reviews). Despite the limited understanding of primary cilia functions, their abundant distribution throughout the brain and correlation of cilia dysfunctions to some cognitive diseases and behavioral abnormalities suggest an essential role for cilia in brain functions. A few G protein-coupled receptors (GPCRs) have been shown to selectively localize to cilia including somatostatin receptor 3 (SSTR3), serotonin receptor 6 (5HTR6), and melanocortin receptors (MC4R) [9, 15, 27, 37, 59, 81].

We recently showed that dysregulations of cilia genes, including ciliary GPCRs, are associated with major psychiatric disorders, including schizophrenia, autism, major

depressive disorder, and bipolar disorder [3]. Therefore, MCHR1 localization on cilia membranes might be the basis of the uniqueness of these receptors in regulating ciliary signaling. In support of this notion, in vitro studies demonstrated that MCH treatment shortened the length of cilia in human retinal pigmented epithelial (hRPE1) cells transfected with MCHR1. Additionally, the reduction in cilia length was mediated via Gi/o-Akt pathway [75]. A recent study by the Saito group demonstrated that treatment of hippocampus slice cultures with MCH induced cilia shortening in the CA1 region [43]. Moreover their results revealed a marked increase in MCH mRNA expression in the lateral hypothalamus of fasting mice which correlated with a reduction of MCHR1-positive cilia lengths in the hippocampal CA1 region [43]. Therefore, we aim to establish the causal relationship between MCH system signaling and cilia length. We examined how manipulating the MCH system affects cilia integrity in multiple mouse brain regions. We used multiple techniques to manipulate the MCH system, including pharmacological, genetic, optogenetic, and chemogenetic approaches to determine how alterations in the MCH system affect cilia length.

Material and Methods

Ex Vivo *Studies*

Rat Brain Slice Culture from the Striatum (Caudate/Putamen (CPu)) and Prefrontal Cortex (PFC)—For rat brain slices, Wistar rats (Charles River Japan, Yokohama, Japan) were maintained in a room under a 12 h light: 12 h darkness cycle and controlled temperature (23 to 25 °C), with water and food available ad libitum. All experimental protocols were reviewed by Hiroshima University Animal Care Committee and met the Japanese Experimental Animal Research Association standards, as defined in the Guidelines for Animal Experiments (1987). We established rat CPu and PFC slice culture method for clear detection of primary cilia and ciliary MCHR1 based on a previous study [43]. The 11-day-old rats were anesthetized with 5% isoflurane and decapitated for slice culture preparation. Brains were removed, embedded in agarose, and dissected into 200 μm coronal slices using a McIlwain tissue chopper (The Mickle Laboratory Engineering, Surrey, UK). The CPu and PFC (Paxinos, 2007) slices were trimmed from the same individual brain slice in ice-cold dissection buffer (2.5 mM KCl, 0.05 μM CaCl2, 1.7 mM NaH2PO4, 11 mM glucose, 20 mM HEPES, 8 mM NaOH, 18 mM NaCl, 0.23 M sucrose, and penicillin G sodium/streptomycin sulfate (PG/SM)). The four CPu slices and eight PFC slices were placed on separate Millicell Cell Culture inserts (PICM0RG50; Merck Millipore, Germany) in 35-mm petri dishes. Each 35-mm petri dish contained 1 ml of starter medium comprising 50% MEM (GIBCO, Grand Island, NY, USA), 25% normal horse serum, 25% Hanks' balanced salt solution, 36 mM glucose, and PG/SM. CPu and PFC slices were placed on each membrane and maintained at 37 °C in a 5% CO_2 incubator. After 1 day, the medium was changed to neurobasal medium (21,103–049; Gibco) containing 1.2% B27 serum-free supplement (17,504–044; Gibco), 25 mM GlutaMAX I (Gibco), and PG/SM (Slice-GM). One-third of the Slice-GM was changed every 72 h. CPu and PFC slices were treated with MCH (30 nM, Peptide Research Institute, Osaka, Japan) on days 14 and 7 of culture, respectively. Immunohistochemical staining of each slice was performed by placing Millicell Cell Culture inserts in 6-well culture plates. After MCH treatment, the slices were fixed for

3 h at 4 °C in fresh 4% paraformaldehyde, washed with PBS, heated (70 °C for 20 min) in 10% Histo VT One (Nacalai Tesque, Kyoto, Japan) in PBS for antigen retrieval, and blocked with PBS containing 5% horse serum and 0.1% Triton X-100 for 2 h. The slices were then incubated with rabbit anti-rat adenylate cyclase 3 (ADCY3, RPCA-ACIII; Encor Biotechnology, Alachua, FL, USA; 1:5000) and goat anti-human MCHR1 (goat anti-human MCHR1; C-17, sc-5534; Santa Cruz Biotechnology; 1:300) primary antibodies overnight at 4 °C. The bound antibodies were detected by incubation with Alexa Fluor 488-conjugated donkey anti-rabbit IgG (A21206, Thermo Fisher Scientific, Rockford, IL, USA; 1:300) or Alexa Fluor 546-conjugated donkey anti-goat IgG (A11056, Thermo Fisher Scientific; 1:300) secondary antibodies for 2 h at room temperature. Each brain slice was cut out from the Millicell Cell Culture inserts using a scalpel together with the Millicell membrane and then mounted with VECTOR Shield.

Microscopic Images and Analysis—The length of primary cilium, which labeled both with MCHR1/ADCY3, was measured with a BZ-9000 fluorescence microscope (Keyence, Osaka, Japan) using PhotoRuler ver. 1.1 software (the Genus Inocybe, Hyogo, Japan). A minimum of 80 cilia per treatment were obtained from at least three independent experiments, and the values are presented as means ± SEM. Numerical data are shown as scatter plot (boxplots and bee swarms) for the cilia length distributions in each group.

In Vivo *Studies*

All experimental procedures were approved by the Institutional Animal Care and Use Committee of the University of California, Irvine, and were performed in compliance with national and institutional guidelines for the care and use of laboratory animals. Animal genetic background and treatments are summarized in Table 1.

Pharmacological Manipulations

Chronic Intracerebroventricular (i.c.v) Administration of MCH: Eight-week-old Swiss Webster male mice ($n = 16$) underwent stereotaxic surgery to implant a stainless steel guide cannula into the lateral ventricles (20-gauge guide cannulas with 2.5-mm custom-cut depth, PlasticsOne). Animals were anesthetized with 2% isoflurane anesthesia (Institutional Animal Care and Use Committee guidelines) and were secured in a Kopf stereotaxic instrument. Guide cannula was implanted at −0.22 mm posterior to bregma, 1.0 mm lateral, and 2.3 mm below the skull surface (G. Paxinos, 2001). Animals were then allowed to recover for 1 week with a dummy cannula in place before injections. Animals were then infused with either vehicle (phosphate-buffered saline (pH 7.4)) with 0.2% bovine serum albumin or MCH peptide (1 nmol) dissolved in the same vehicle for 7 consecutive days using a 50 μl Hamilton Microsyringe. MCH (1 nmol) was dissolved in phosphate-buffered saline (pH 7.4) with 0.2% bovine serum albumin. The dose of MCH was determined by previously reported findings [70]. Following the last injection, 9–10-week-old mice were anesthetized with isoflurane and perfused intracardially with saline and 4% paraformaldehyde.

Intraperitoneal Administration of MCHR1 Antagonist GW 803,430: Eight-week Swiss Webster male mice were administered intraperitoneally (i.p.) 3 mg/kg ($n = 8$) MCH1R

antagonist GW803430 or vehicle ($n = 8$) for 7 consecutive days [31, 70]. GW80343 was dissolved in vehicle made in 2% Tween 80 with acetic acid. This dose was selected based on previous receptor occupancy studies demonstrating that near-complete blockade of the MCH system is achieved following i.p. administration at the 3 mg/kg dose [31, 70]. Following the final injection at 9–10 weeks old, animals were perfused transcardially for tissue fixation.

Genetic Manipulation

Germline MCHR1 Knockout (MCHR1 KO) and MCH Conditional Knockout (MCH-cKO) mice: MCHR1 KO male mice were generated as previously described [49]. Pmch-Cre/ + ,iDTR/$^{+}$ mice were generated as described previously [2]. Briefly, PmchCre mice (Tg(pMCH-cre)1Lowl/J mice, Jackson Laboratories, Bar Harbor, Maine, USA) that express Cre-recombinase (Cre) under the MCH promoter [45] were bred with homozygous inducible diphtheria toxin receptor iDTR/$^{+}$ mice (from Dr. Satchidananda Panda and originally generated in the lab of Dr. Ari Waisman), rendering MCH neurons in these mice sensitive to diphtheria toxin (DT) [2, 17, 70, 83]. The resulting iDTR^{+}PmchCre^{+} (iDTR^{+}/Cre^{+}) and their control littermate iDTR^{+}PmchCre^{-}(iDTR^{+}/Cre^{-}) mice were injected twice in 4 days with the diphtheria toxin (DT) (16 μg/kg, i.p.), which then produces profound ablation of MCH neurons.

Optogenetic Stimulation of MCH Neurons

Surgery: AAV5-EF1a-DIO-ChR2-T159c-eYFP (titer, ≥ 1×10^{13} vg/mL) is an EF1a-driven, Cre-dependent, humanized channelrhodopsin E123T/T159C mutant fused to EYFP for optogenetic activation (pAAV-Ef1a-DIO hChR2 (E123T/T159C)-EYFP was a gift from Karl Deisseroth (Addgene viral prep # 35,509-AAV5; http://n2t.net/addgene:35509; RRID: Addgene_35509) [50]. AAV5-EF1a-DIO-ChR2-T159c-eYFP was stereotaxically injected into the lateral hypothalamus (flat skull coordinates from bregma: anteroposterior, – 1.30 mm; mediolateral, + 1 mm; and dorsalventral, – 5.20 mm) of 8-week-old male transgenic C57BL/6 PmchCre + ($n = 8$) and PmchCre− animals ($n = 8$), (Jackson Laboratories, Bar Harbor, Maine, USA) that express Cre-recombinase (Cre) under the MCH promoter. Each mouse received one injection of 800 nl in each lateral hypothalamus. At this time, the high-power LED fiber cannula (core diameter 200 μm, outer diameter 225 μm, length 2.5 mm, numerical aperture 0.66, Prizmatix, Israel) was implanted in the lateral hypothalamus at – 5.0 mm slightly above the injection site. The cannula light irradiance was adjusted to 6 mW before implantation. An additional hole was drilled on the opposite side for stainless steel holding screws. The fiber was fixed with dental cement holding the fiber and screw to the skull. The skin was closed with silk sutures. Animals were allowed to recover for 1 week before the start of the experiments. Correct fiber placement and injection site were ascertained postmortem on coronal brain sections.

Animals were habituated to the connection of the fiber patch cords to their cannulas inside their home cage for 1 h for 3 days. On the fourth day, animals were connected to the fiber patch cord and were tested in their home cage on feeding behavior. Animals were exposed to a 460 nm blue led light source to excite ChR2 at a specific stimulation paradigm: 10 Hz, 10 ms pulse 1 s, repeated every 4 s for 10 min. Feeding behavior was tracked and recorded (Fig. S1). Twenty-four hours after feeding behavior test, mice were exposed to blue light at

10 ms pulse 1 s repeated every 4 s for 30 min and were intracardially perfused 90 min post light exposure.

Designer Receptors Exclusively Activated by Designer Drug (DREADD)-Based Chemogenetic Stimulation of MCH Neurons—AAV8-hSyn-DIO-hM3D(Gq)-mCherry (titer, 4.8×10^{12} GC/mL) (pAAV-hSyn-DIO-hM3D(Gq)-mCherry was a gift from Bryan Roth (Addgene viral prep #44,361-AAV8; http://n2t.net/addgene: 44,361; RRID:Addgene_44361)) was stereotaxically injected into the lateral hypothalamus (flat skull coordinates from bregma: anteroposterior, – 1.30 mm; mediolateral, ± 1 mm; and dorsal ventral, – 5.20 mm) (G. Paxinos, 2001) of 8-week-old male transgenic C57BL/6 PmchCre + ($n = 8$) and PmchCre− animals ($n = 8$). This virus is a Syn-driven, Cre-dependent, hM3D(Gq) receptor with an mCherry reporter for CNO-induced neuronal activation [46]. Using this virus in mice that express Cre in MCH neurons allows precise expression of DREADD in the lateral hypothalamus and activate MCH neurons directly via CNO. Mice received two injections (both hemispheres; 0.6 nl), and then 1 week post-surgery animals were injected with one dose of CNO (1 mg/kg) and perfused 90 min after CNO injection.

Immunohistochemistry—Immunofluorescent staining was carried out as previously reported [65]. Briefly, 9–10-week-old animals were perfused transcardially under isoflurane anesthesia with saline followed by 4% paraformaldehyde in phosphate buffer saline. Brains were removed, and 30 μm coronal brain sections were dissected. The MCH-neuron ablation was verified by visualizing MCH neurons using rabbit polyclonal anti-MCH antibody (1:150,000, antibody courtesy of W. Vale, Salk Institute, La Jolla, CA, USA) as previously described [70]. A goat anti-rabbit (1:500,Thermo Fisher) was used to visualize MCH immunoreactivity. For the cilia study, three to five sections were selected from each region of interest according to the mouse brain atlas (G. Paxinos, 2001). Primary cilia were stained with ADCY3 (rabbit, 1:500; Santa Cruz Biotechnology) and the secondary antibody donkey anti-rabbit Alexa 546 (Thermo Fisher Scientific). For c-Fos immunohistochemistry, mice were perfused 90 min after stimulation, and brain sections were stained with rabbit anti-c-Fos antibody (1:500, Invitrogen). Nuclei were stained with 4′,6-diamidino-2-phenylindole (DAPI) solution (1:10,000) and mounted with Aqua-mount mounting solution. Four to six brains from each group were used for quantification. For each brain, we used four to six non-consecutive sections per region of interest. Quantification of primary cilia was based solely on ADCY3 immunofluorescence positive signals. Each section was imaged bilaterally, thus giving 2 images quantifying a total of 10 images per region per brain. Cilia were counted in the bilateral areas of each section, and each brain was given one averaged cilia length value for each region. Image acquisition was carried out using confocal laser microscope. Images were captured using Leica Sp8 TCS confocal microscope (UCI optical biology core facility). Cilia length was measured using ImageJ [71] in all cells in each section, and the mean values of three sections per brain of 3–5 brains were calculated. A number of cilia in specific regions of the brain were also counted and referred to as cilia density per field. All cilia measurements were performed by two persons blind to the experiment conditions using cilia length cutoff of 0.5 μm. A total of 16 animals were used per experiment (8 control and 8 experimental groups), and 3–5 animals per group were used

for analysis. Additional animals were used to account for any margins of error that may occur during perfusions, cutting, etc.

Statistical Analysis

GraphPad Prism (GraphPad Software, Inc.) was used for statistical analysis, and all data were presented as mean ± standard error mean (SEM). Student's unpaired *t* test was used to analyze the results. *P* value < 0.05 was considered statistically significant.

Results

MCH Shortens Cilia Length in the Rat Organotypic Striatum and Prefrontal Cortex Culture

Immunohistochemical analyses in the brains of rats showed that ADCY3/MCHR1 double-positive neuronal primary cilia were localized in discrete regions, including CPu and cerebral cortex [26]. Cilia MCHR1 merge with ADCY3 was also observed in cultured slices derived from the rat CPu and PFC (Fig. 1a, c). The neuronal cilia length in the CPu slices was 10.30 ± 0.23 μm (mean ± SEM), and MCH treatment for 18 h decreased this length by 23.0% (7.90 ± 0.28 μm, unpaired *t* test, $P < 0.01$) (Fig. 1b). We observed a similar effect of MCH in rat PFC slice cultures. Exposure to MCH led to neuronal cilia shortening by 31% (4.39 ± 0.12 μm vs 3.05 ± 0.06 μm; mean ± SEM, unpaired *t* test, $P < 0.01$) (Fig. 1d).

Activation of the MCH System Shortens Cilia Length in the Mouse Brain

MCHR1 Agonist Shortens Cilia in the Mouse Brain—The central (i.c.v.) administration of MCH in adult mice for 7 consecutive days caused a significant decrease in the cilia length in several regions of the brain, including the hippocampus, striatum, prefrontal cortex (PFC), and nucleus accumbens (NAc) (Fig. 2a). In the PFC, administration of MCH caused a 42% reduction in cilia length (4.96 ± 0.30 μm in the PFC of the animals administered vehicle, $n = 4$, compared to 2.85 ± 0.1 μm in mice treated with MCH, $n = 4$, $t = 6.433$, $P = 0.0007$, unpaired *t* test) (Fig. 2b-d). In the CA1, administration of MCH caused a 33% shortening in cilia length (10.18 ± 0.30 μm in the CA1 of the animals administered vehicle, $n = 4$, compared to 6.743 ± 0.23 μm in mice treated with MCH, $n = 4$, $t = 8.436$, $P = 0.0002$, unpaired *t* test) (Fig. 2e-g). In the CPu, administration of MCH, $n = 5$, caused a 37% reduction in cilia length (5.04 ± 0.17 μm compared to 8.005 ± 0.2 μm in the CPu of the animals administered vehicle, $n = 5$, $t = 10.03$, $P < 0.0001$, unpaired *t* test) (Fig. 2h-j). In the NAc, administration of MCH caused a reduction in cilia length by 32% (8.287 ± 0.67 μm in the NAc of the animals administered vehicle, $n = 4$, compared to 5.566 ± 0.33 μm when given MCH, $n = 4$, $t = 3.648$, $P = 0.0107$, unpaired *t* test) (Fig. 2k-m). Chronic MCH administration caused a significant decrease in cilia density per field in the PFC ($t = 3.849$, $P = 0.0085$), CA1 ($t = 3.141$, $P = 0.02$), CPu ($t = 4.224$, $P = 0.0055$), and NAc ($t = 3.766$, $P = 0.0093$) (Fig. S2).

Optogenetic and Chemogenic Excitation of MCH Neurons Shortens Cilia Length—Optogenetic stimulation of MCH neurons was applied to one hemisphere of the brain at 460 nm blue led light at 10 Hz 10 ms pulse 1 s repeated every 4 s for 10 min, based on previously reported rates, at which MCH neurons fire [33, 39] (Fig. 3a). Expression of ChR2 in the LH MCH neurons was confirmed using double immunostaining of GFP

(green) and MCH (red) in Pmch-Cre + and PmchCre− mice (Fig. 3b). Co-expression of GFP fluorescence (green) and c-Fos immunofluorescence (red) identifies cells recently activated neurons in PmchCre + and PmchCre− mice (Fig. 3c). optogenetic stimulation of MCH neurons in PmchCre + mice caused a significant bilateral decrease in cilia length compared to PmchCre− mice (control) in the CA1, striatum, PFC, and NAc. In the PFC, cilia lengths were shortened by 59% in PmchCre + mice compared to PmchCre− following optogenetic stimulation of MCH neurons (6.497 ± 0.6 μm in PmchCre− mice, $n = 4$, compared to 2.635 ± 0.23 μm in PmchCre + mice, $n = 4$, $t = 6.319$, $P = 0.0007$, unpaired t test) (Fig. 3d-f). In the CA1, stimulating MCH neurons caused a significant reduction in cilia length by 34% (3.823 ± 0.33 μm in PmchCre− mice, $n = 4$, compared to 2.536 ± 0.14 μm in PmchCre + mice, $n = 4$, $t = 3.535$, $P = 0.0123$, unpaired t test) (Fig. 3g-i). In the CPu, stimulating MCH neurons caused a significant shortening of cilia length by 56% (6.065 ± 0.45 μm in PmchCre− mice, $n = 5$ compared to 4.031 ± 0.4 μm in PmchCre + mice, $n = 5$, $t = 3.520$, $P = 0.0078$, unpaired t test (Fig. 3k-l). In the NAc stimulating MCH neurons caused significant reduction in cilia length by 20% (7.442 ± 0.46 μm in PmchCre− mice, $n = 4$, compared to 5.952 ± 0.34 μ in PmchCre + mice, $n = 4$, $t = 2.593$, $P = 0.0410$, unpaired t test) (Fig. 3m-o). PmchCre + mice also exhibited more food intake than PmchCre− mice when exposed to blue light. Over the observed 10 min, PmchCre + mice averaged 74.13 s of feeding, while PmchCre− mice averaged 7.413 s ($t = 7.027$, $P < 0.001$) (Fig. S1). Stimulating MCH neurons via optogenetics caused a significant decrease in cilia density per field in the PFC ($t = 3.789$, $P = 0.0091$), CA1 ($t = 6.324$, $P = 0.0007$), and CPu ($t = 5.656$, $P = 0.0013$) (Fig. S3).

DREADD expression in MCH neurons was confirmed by double immunostaining of mCherry fluorescence (red) identifying DREADD-expressing neurons and MCH staining (green) (Fig. 4a,b). Co-expression of mCherry fluorescence (red) identifies DREADD-expressing neurons, and c-Fos immunofluorescence (green) confirmed cells recently activated in PmchCre + and PmchCre− mice (Fig. 4c). DRE-ADD hM3Dq-mediated chemogenic activation of MCH neurons in PmchCre + adult mice caused a significant decrease in cilia length compared to PmchCre− adult mice in both hemispheres of the brain in several regions of the brain, including the CA1, striatum, PFC, and NAc. In the PFC, stimulating MCH neurons in PmchCre− mice caused a 40% decrease in cilia length (5.226 ± 0.4111 μm in PmchCre− mice, $n = 4$, compared to 3.125 ± 0.3080 μm in PmchCre + mice, $n = 4$, $t = 4.090$, $P = 0.0064$, unpaired t test) (Fig. 4d-f). In the CA1, stimulating MCH neurons in PmchCre− mice caused a 39% decrease in cilia length (6.079 ± 0.3029 μm in PmchCre− mice, $n = 4$, compared to 3.699 ± 0.3173 μm in PmchCre + mice, $n = 4$, $t = 5.426$, $P = 0.0016$, unpaired t test) (Fig. 4g-i). In the CPu, stimulating MCH neurons in PmchCre− mice caused a 40% decrease in cilia length (6.792 ± 0.3493 μm in PmchCre− mice, $n = 4$, compared to 4.059 ± 0.4322 μm in PmchCre + mice, $n = 4$ ($t = 4.918$, $P = 0.0027$, unpaired t test) (Fig. 4j-l). In the NAc, stimulating MCH neurons in PmchCre− mice caused a 32% decrease in cilia length (9.240 ± 0.4591 μm in PmchCre− mice, $n = 4$, compared to 6.267 ± 0.1699 μm in PmchCre + mice, $n = 4$, $t = 6.073$, $P = 0.0009$, unpaired t test) (Fig. 4m-o). Activation of MCH neurons via chemogenetics caused a significant decrease in cilia density per field in the PFC ($t = 4.092$, $P = 0.0064$) and CA1 ($t = 3.613$, $P = 0.0112$) (Fig. S4).

Inactivation of the MCH System Increases Cilia Length in the Mouse Brain

MCHR1 Antagonist Lengthens Cilia—The administration of GW803430 via intraperitoneal injection in adult mice for 7 consecutive days caused a significant increase in the cilia length in multiple brain regions, including the CA1 of the CA1, striatum, PFC, and NAc (Fig. 5a). Administration of GW803430 caused an increase in cilia length in the PFC by 42% (3.935 ± 0.42 μm in the PFC of the animals administered vehicle, $n = 4$, compared to 6.845 ± 0.3 μm in mice treated with GW803430, $n = 4$, $t = 5.646$, $P = 0.0013$, unpaired t test) (Fig. 5b-d). GW803430 administration caused an increase in cilia length in the CA1 by 28% (6.103 ± 0.5 μm in the animals administered vehicle, $n = 4$, compared to 8.595 ± 0.55 μm in mice treated with GW803430, $n = 4$, $t = 3.4$, $P = 0.0145$, unpaired t test) (Fig. 5e-g). The administration of GW803430 caused lengthening in cilia in the CPu by 33% (7.30 ± 0.50 μm, $n = 4$, compared to 4.84 ± 0.24 μm in the CPu of the animals administered vehicle, $n = 4$, $t = 4.583$, $P = 0.0038$, unpaired t test) (Fig. 5h-j). GW803430 increased cilia length in the NAc by 17% (7.544 ± 0.22 μm in the NAc of the animals administered vehicle, $n = 4$, compared to 9.190 ± 0.17 μm in mice treated with GW803430, $n = 4$, $t = 5.992$, $P = 0.0010$, unpaired t test (Fig. 5k-m). Administration of GW803430 resulted in no significant difference in cilia density per field in the PFC, CA1, CPu, and NAc (Fig. S5).

Cilia Length Is Increased in MCH- and MCHR1-Deficit Mice—To assess MCH-neuron ablation extent following DT injection into IDTR + PmchCre− and IDTR + PmchCre− mice, MCH neurons were visualized and counted using rabbit polyclonal anti-MCH antibody (Fig. 6a,b), and only mice that exhibited over 90% ablation of MCH neurons were used in the study. The conditional ablation of MCH neurons in adult mice (MCH-cKO) caused a significant increase in the cilia length in several regions of the brain including CA1, striatum, and PFC and NAc (Fig. 6a,b). In the PFC of MCH-cKO mice, cilia length increased by 19% (5.03 ± 0.32 μm in IDTR + Pmch-Cre− mice, $n = 3$, compared to 6.185 ± 0.04609 μm in IDTR + PmchCre + mice, $n = 3$ $t = 3.539$, $P = 0.024$, unpaired t test) (Fig. 6c-e). In the CA1 of IDTR + MCH-cKO mice, cilia length increased by 24% (6.24 ± 0.23 μm in IDTR + PmchCre− mice, $n = 3$, compared to 8.209 ± 0.07566 μm in IDTR + PmchCre + mice, $n = 3$, $t = 8.265$, $P = 0.0012$, unpaired t test) (Fig. 6f-h). In the CPu of MCH-cKO mice, cilia length increased by 29% (5.242 ± 0.2518 μm IDTR + PmchCre− mice, $n = 3$, compared to 7.373 ± 0.6131 μm in IDTR + PmchCre + mice, $n = 3$ ($t = 3.215$, $P = 0.0324$, unpaired t test) (Fig. 6i-k). In the NAc of MCH-cKO mice, cilia length increased by 23% (5.239 ± 0.4177 μm in IDTR + PmchCre− mice, $n = 3$, compared to 6.823 ± 0.3695 μm in IDTR + Pmch-Cre + mice, $n = 3$ ($t = 2.841$, $P = 0.0456$, unpaired t test) (Fig. 6l-n). MCH-cKO mice resulted in a significant increase in cilia density per field in the CA1 ($t = 6.516$, $P = 0.0006$) and the NAc ($t = 5.047$, $P = 0.0023$) (Fig. S7).

Germline deletion of MCHR1 in mice caused a significant increase in the cilia length in several brain regions, including CA1, CPu, PFC, and NAc. In the PFC of MCHR1 KO mice, there was an increase in cilia length by 41% (3.8 ± 0.1 μm in WT mice, $n = 4$, compared to 6.50 ± 0.09 μm in the MCHR1KO mice, $n = 5$, $t = 20.15$, $P < 0.0001$, unpaired t test) (Fig. 7a-c). In the CA1 of the hippocampus of MCHR1 KO mice, cilia were 22% longer than in WT mice (2.8 ± 0.03 μm in the CA1 of the WT mice, $n = 4$, compared to 3.6 ± 0.10 μm. 0.1 μm in the MCHR1KO mice, $n = 5$, $t = 6.712$, $P = 0.0003$, unpaired t test) (Fig. 7d-f). In the

CPu of the MCHR1 KO mice, $n = 5$, cilia length increased by 17% (9.5 ± 0.3 μm compared to 7.9 ± 0.3 μm in WT mice, $n = 4$, $t = 3.952$, $P = 0.005$, unpaired t test) (Fig. 7g-i). In the NAc of the MCHR1 KO mice, cilia length increased by 25% (7.60 ± 0.50 μm in the NAc of the WT mice, $n = 4$, compared to 10.19 ± 0.50 μ in MCHR1KO mice, $n = 5$, $t = 4.434$, $P = 0.003$, unpaired t test) (Fig. 7j-l). MCHR1KO mice caused a significant increase in cilia density per field in the CA1 ($t = 3.884$, $P = 0.0081$) (Fig. S6).

Discussion

In this study, we established the causal effects of MCH signaling pathways on cilia length. We first showed that MCH treatment causes cilia shortening in the striatal and cortical brain slice cultures. We then demonstrated that the stimulation of the MCH system through direct agonist activation of the MCHR1 or via optogenetic and chemogenic excitation of MCH neurons causes a significant decrease in cilia length. In contrast, the inactivation of the MCH system through pharmacological blockade of MCHR1 or genetic manipulation (MCHR1 germline deletion or MCH neurons' conditional ablation) causes a significant increase in cilia length.

MCHR1 is widely distributed throughout the brain, with high density in the CPu, NAc, CA1 of the hippocampus, and the PFC [40, 68]. Therefore, we focused on these regions in examining the effects of MCH system activation and inactivation on cilia length. Consistent with previous reports, we found that cilia length differed among brain regions [11, 36, 43, 51, 74]. Interestingly, we also found that cilia length differs among mouse strains. This observation warrants further investigation to determine whether such variabilities in cilia length correlate with genotypic or phenotypic characteristics of these different strains.

The various manipulation approaches allowed us to (1) recapitulate conditions used previously to substantiate MCH physiological functions; (2) differentiate between the effects of MCH neurons and MCHR1 manipulation; (3) distinguish the effects of acute versus chronic activation/inactivation of MCH system; and (4) determine the effects of early-life versus adult stage MCH system manipulations.

The role of MCH in regulating a wide variety of physiological functions such as feeding, obesity, reward, and sleep has been established using pharmacological and genetic manipulations [19, 20, 30, 41, 73]. For example, central chronic infusions of MCH had long been shown to induce mild obesity in wild-type mice [32], In contrast, subchronic administration of MCHR1 antagonists and MCHR1/MCH genetic deletion are known to produce anti-obesity effects in mice [31, 49]. The ciliopathy Bardet–Biedl syndrome (BBS) is characterized by obesity, and mutations affecting the mouse orthologs of BBS-associated genes disrupt the localization of MCHR1 [9, 87]. Thus, failure of MCHR1 to reach the cilium could potentially be associated with failure in the MCHR1 signaling pathway in the cilia, leading to obesity in BBS [28, 77].

Given that MCH neurons synthesize and release other neurotransmitters/neuropeptides, including gamma-aminobutyric acid (GABA), neuropeptide E-I (NEI), and neuropeptide G-E (NGE) [53, 61], it is important to distinguish the selective role of the activation of

MCHR1 present on neuronal primary cilia from the activation or inactivation of MCH neurons releasing MCH or other neurotransmitter, in regulating primary cilia length. Hence, MCHR1 pharmacological activation by MCH intracerebral infusion, the blockade of the receptors by GW803430 systemic treatment and MCHR-1 germline deletion, allowed the exploration of the selective role of MCHR1. In parallel, optogenetic and DREADD stimulation of the MCH neurons and IDTR-dependent ablation of MCH neurons allowed for exploring the role of MCH neurons. Optogenetics and DREADD technologies have also been previously used to explore MCH neurons' role in sleep, reward, and feeding [12, 25, 52].

Previous reports demonstrated distinctive effects of acute versus chronic activations of MCH systems on body weight [72]. Therefore, we examined the effects of acute (optogenetic and chemogenetic stimulation) and chronic activations (MCH i.c.v. administration for 7 days) of the MCH system on cilia length. We previously showed that developmental and adulthood inactivation of the MCH system in mice leads to distinct behavioral deficits. For example, germline MCHR1 deletion but not adult IDTR-dependent ablation of MCH neurons caused olfactory impairment and social deficits [83]. Therefore, we examined the effects of germline MCHR1 deletion and adulthood conditional MCH ablation on cilia length.

Strikingly, we found that the different MCH system manipulations produced consistent patterns of alterations in cilia length. The activation of MCH system consistently shortened cilia length, while the inactivation of MCH system lengthened cilia length. The findings that both acute and chronic activation of MCH system shortened cilia length and that both early-life and adulthood inactivation of the MCH system lengthened cilia substantiate the dynamic nature of the cilia system and suggest that cilia's morphology undergoes rapid changes in response to its environment. Most importantly, our findings provide the first evidence for the direct and moment-to-moment regulation of the brain cilia structure by the MCH system.

Unexpectedly, unilateral optogenetic stimulation of MCH neurons in the lateral hypothalamus caused bilateral shortening of cilia length in the PFC, CA1, CPu, and NAc. This finding may suggest that MCH neurons project ipsilaterally and contralaterally to these brain regions. Another explanation might be that MCH activation may produce ipsilateral modifications of other neurotransmitter systems, which may result in contralateral shortening of cilia length. It is well-established that MCH neurons innervate serotonergic neurons in the raphe nucleus and regulate the activity of these neurons [24, 78]. Indeed, specific MCH-regulated functions are mediated through the serotonin system [48, 79]. Thus, the activation of MCH neurons may regulate cilia indirectly through its interaction with the serotonin system. Interestingly, MCHR1 and 5-HT6 are among the very few GPCRs that preferentially localize to primary cilia [6], and the inhibition of 5-HT6 receptors is known to shorten cilia length [16, 41]. Another possible explanation for the bilateral modifications of the cilia length could be that the stimulation of MCH neurons induces the release of MCH to the ventricular system, thus allowing MCH to reach distant targets via the cerebrospinal fluid causing cilia shortening throughout the brain [55, 76].

While cilia shortening effects of MCH system activation is not unexpected, and is, indeed, consistent with previous in vitro studies, the effect of MCH signaling on cilia retraction is surprising. However, taking in consideration our threshold that was setup for measuring cilia length (> 0.5 μm), it is possible that MCH system activation reduced cilia length to levels that were below this threshold.

A possible mechanism for MCH-induced cilia shortening is through a Gi/o-dependent Akt pathway [36, 75]. The ciliary MCHR1-Gi/o pathway seems to result in a series of downstream signal cascades that lead to increasing the depolymerization of cytosolic tubulin, increasing soluble tubulin levels in the cell body and increase actin filaments [36, 75]. A very recent study by Dr. Saito group demonstrated that the PDZ and LIM domain-containing protein 5 (PDLIM5) is the most important crucial factor in MCHR1-mediacted cilia shortening and discovered that the actin-binding protein alpha-actinin 1/4 is the main downstream target of the PDLIM5 signaling pathway that mediate MCHR1-induced cilia shortening [26].

Defects in the assembly such as cilia shortening have been shown to cause a range of severe diseases and developmental disorders called ciliopathies, which are associated with neurological deficits such as abnormal cortical formation and cognitive deficits [38, 66, 80]. We have recently shown that brain cilia genes were differentially expressed in major psychiatric disorders, including schizophrenia, autism spectrum disorder, depression, and bipolar disorder [3]. On the other hand, evidence from our own work and others strongly support an essential role for the MCH system, particularly MCHR1, in the pathophysiology of schizophrenia. We showed that MCHR1 mRNA is decreased in the PFC of patients with schizophrenia [83]. We also demonstrated that genetic manipulation of the MCH system via the deletion of MCHR1 and the conditional ablation of MCH neurons resulted in behavioral abnormalities mimicking schizophrenia-like phenotypes, including repetitive behavior, social impairment, impaired sensorimotor gating, and disrupted cognitive functions [84]. We also showed that MCHR1 germline deletion causes alterations in depressive-like behavior that is sex-dependent [83]. These same genetic models were used in our current study to examine the consequences of this genetic manipulation on cilia length. In both IDTR + PmchCre + and MCHR1KO animals, we found a significant increase in cilia in all regions, including the PFC, CA1, CPu, and NAc. Our previous and current data may point to the role of ciliary MCHR1 in the pathophysiology of psychiatric disorders such as schizophrenia and depression. Together, our previous and current studies point at the cilia elongation as a possible mechanism through which MCH system dysregulation causes social and cognitive deficits in mice and is associated with psychiatric disorders in humans [3, 83]. Our results also prompt the question on whether selective targeting of cilia MCHR1 might offer a novel approach to treat psychiatric disorders. Indeed, studies have demonstrated that some pharmacological agents can alter cilia length. For example, lithium, a mood stabilizer that is used in treatment of bipolar disorder and acute mania, increases MCHR1-positive cilia length in several cell types, including neuronal cells, the dorsal striatum, and NAc [51].

Since our analysis of cilia length was mainly based on the quantification of ADCY3 positive signals and not in MCHR-1 positive ones, and given that some brain cilia do not express MCHR1, further studies are needed to determine whether cilia length is regulated by MCH

signaling in MCHR1-expressing neurons that have MCHR1-negative cilia. On the other hand, as our study was conducted on male mice, it is of particular importance to investigate the sex difference in cilia length as a response to MCH system manipulation particularly due to the sexually dimorphic expression of MCH in rodent brain [67]. Given the high dynamic nature of cilia, it would also be interesting to investigate whether the estrous cycle in female mice affects cilia morphology and length.

Unexpectedly, we found that within the same strains, the vehicle-treated animals in the two pharmacological manipulations exhibited different cilia lengths. For example, the average cilia length was 4.84 ± 0.24 μm in the CPU of animals treated with the vehicle of GW803430, compared to 8.005 ± 0.2 μm in animals treated with the vehicle of MCH. While the reasons for these differences in cilia lengths are not fully understood, this finding substantiates the well-established highly dynamic features of cilia structure and morphology [5, 7, 21, 42, 47, 54, 56, 57, 86]. Given that the control animals, despite being from the same sex, strain, and age, underwent different experimental procedures, the variability in cilia length among the control animals might be attributed to factors related to the experimental designs. Some of these factors might be (1) the composition of vehicles administered, (2) the route of administration, and (3) the exposure to stereotactic surgery and anesthetic agents. First, while the MCH vehicle was composed of phosphate-buffered saline with 0.2% bovine serum albumin, GW803430 dissolving vehicle was composed of 2% Tween 80 with acetic acid. Second, since MCH does not cross the blood–brain barrier, intracerebroventricular route was used for direct injection of MCH into the cerebrospinal fluid in the ventricles. MCHR1 antagonist GW803430, on the other hand, was administered via intraperitoneal route. The vehicles and routes of administration were selected based on previously characterized pharmacological and behavioral profiles [1, 70]. Lastly, unlike the animals injected with GW803430, MCH-injected animals underwent stereotactic surgery for cannula implantation and had been administered isoflurane to induce anesthesia. These factors may have contributed to the variability in cilia lengths in the control animals,thus, further investigation is necessary to determine whether these effects are sufficient to influence changes in cilia length.

In conclusion, our present study has established the causal regulatory effects of the MCH system signaling on cilia length. The findings of this study are significant because (1) they show for the first time in vivo that primary cilia length can be regulated by the MCH signaling, proving the link between GPCRs and cilia length regulation and (2) they implicate ciliary MCHR1 as a potential therapeutic target for the treatment of pathological conditions characterized by impaired cilia function.

Supplementary Material

Refer to Web version on PubMed Central for supplementary material.

Acknowledgements

The authors would like to thank Dr. Olivier Civelli for the helpful discussions.

Funding

The work of SN and AA was supported in part by R01-HL147311-02S1.

Data Availability

Data that support the findings of this study are available from the corresponding author upon request.

References

1. Alachkar A, Alhassen L, Wang Z, Wang L, Onouye K, Sanathara N, Civelli O (2016) Inactivation of the melanin concentrating hormone system impairs maternal behavior. European neuropsychopharmacology: the journal of the European College of Neuropsychopharmacology 26:1826–1835 [PubMed: 27617778]
2. Alhassen L, Phan A, Alhassen W, Nguyen P, Lo A, Shaharuddin H, Sanathara N, Civelli O, Alachkar A (2019) The role of olfaction in MCH-regulated spontaneous maternal responses. Brain Res 1719:71–76 [PubMed: 31121161]
3. Alhassen W, Chen S, Vawter M, Robbins BK, Nguyen H, Myint TN, Saito Y, Schulmann A, Nauli SM, Civelli O et al. (2021) Patterns of cilia gene dysregulations in major psychiatric disorders. Prog Neuropsychopharmacol Biol Psychiatry 109:110255 [PubMed: 33508383]
4. Arletti R, Benelli A, Bertolini A (1992) Oxytocin involvement in male and female sexual behavior. Ann N Y Acad Sci 652:180–193 [PubMed: 1626828]
5. Atkinson KF, Sherpa RT, and Nauli SM (2019). The role of the primary cilium in sensing extracellular pH. Cells 8.
6. Bansal R, Engle SE, Antonellis PJ, Whitehouse LS, Baucum AJ 2nd, Cummins TR, Reiter JF, Berbari NF (2019) Hedgehog pathway activation alters ciliary signaling in primary hypothalamic cultures. Front Cell Neurosci 13:266 [PubMed: 31249512]
7. Bargmann CI (2006). Chemosensation in C. elegans. Worm-Book: the online review of C. elegans biology, 1–29.
8. Berbari NF, Johnson AD, Lewis JS, Askwith CC, Mykytyn K (2008) Identification of ciliary localization sequences within the third intracellular loop of G protein-coupled receptors. Mol Biol Cell 19:1540–1547 [PubMed: 18256283]
9. Berbari NF, Lewis JS, Bishop GA, Askwith CC, Mykytyn K (2008) Bardet-Biedl syndrome proteins are required for the localization of G protein-coupled receptors to primary cilia. Proc Natl Acad Sci USA 105:4242–4246 [PubMed: 18334641]
10. Berbari NF, O'Connor AK, Haycraft CJ, Yoder BK (2009) The primary cilium as a complex signaling center. Current biology: CB 19:R526–535 [PubMed: 19602418]
11. Bishop GA, Berbari NF, Lewis J, Mykytyn K (2007) Type III adenylyl cyclase localizes to primary cilia throughout the adult mouse brain. J Comp Neurol 505:562–571 [PubMed: 17924533]
12. Blanco-Centurion C, Liu M, Konadhode RP, Zhang X, Pelluru D, van den Pol AN, Shiromani PJ (2016) Optogenetic activation of melanin-concentrating hormone neurons increases non-rapid eye movement and rapid eye movement sleep during the night in rats. Eur J Neurosci 44:2846–2857 [PubMed: 27657541]
13. Blouin AM, Fried I, Wilson CL, Staba RJ, Behnke EJ, Lam HA, Maidment NT, Karlsson KAE, Lapierre JL, Siegel JM (2013) Human hypocretin and melanin-concentrating hormone levels are linked to emotion and social interaction. Nat Commun 4:1547 [PubMed: 23462990]
14. Borowsky B, Durkin MM, Ogozalek K, Marzabadi MR, DeLeon J, Lagu B, Heurich R, Lichtblau H, Shaposhnik Z, Daniewska I et al. (2002) Antidepressant, anxiolytic and anorectic effects of a melanin-concentrating hormone-1 receptor antagonist. Nat Med 8:825–830 [PubMed: 12118247]
15. Brailov I, Bancila M, Brisorgueil MJ, Miquel MC, Hamon M, Verge D (2000) Localization of 5-HT(6) receptors at the plasma membrane of neuronal cilia in the rat brain. Brain Res 872:271–275 [PubMed: 10924708]

16. Brodsky M, Lesiak AJ, Croicu A, Cohenca N, Sullivan JM, Neumaier JF (2017) 5-HT6 receptor blockade regulates primary cilia morphology in striatal neurons. Brain Res 1660:10–19 [PubMed: 28087224]

17. Buch T, Heppner FL, Tertilt C, Heinen TJ, Kremer M, Wunderlich FT, Jung S, Waisman A (2005) A Cre-inducible diphtheria toxin receptor mediates cell lineage ablation after toxin administration. Nat Methods 2:419–426 [PubMed: 15908920]

18. Chaki S, Funakoshi T, Hirota-Okuno S, Nishiguchi M, Shimazaki T, Iijima M, Grottick AJ, Kanuma K, Omodera K, Sekiguchi Y et al. (2005) Anxiolytic- and antidepressant-like profile of ATC0065 and ATC0175: nonpeptidic and orally active melanin-concentrating hormone receptor 1 antagonists. J Pharmacol Exp Ther 313:831–839 [PubMed: 15677346]

19. Chung S, Hopf FW, Nagasaki H, Li CY, Belluzzi JD, Bonci A, Civelli O (2009) The melanin-concentrating hormone system modulates cocaine reward. Proc Natl Acad Sci USA 106:6772–6777 [PubMed: 19342492]

20. Chung S, Verheij MM, Hesseling P, van Vugt RW, Buell M, Belluzzi JD, Geyer MA, Martens GJ, Civelli O (2011) The melanin-concentrating hormone MCH system modulates behaviors associated with psychiatric disorders. PloS one 6:e19286 [PubMed: 21818251]

21. Clary-Meinesz CF, Cosson J, Huitorel P, Blaive B (1992) Temperature effect on the ciliary beat frequency of human nasal and tracheal ciliated cells. Biol Cell 76:335–338 [PubMed: 1305479]

22. Cohen H, Liberzon I, Matar MA (2014) Translational implications of oxytocin-mediated social buffering following immobilization stress in female prairie voles. Biol Psychiat 76:268–269 [PubMed: 25060784]

23. Della-Zuana O, Presse F, Ortola C, Duhault J, Nahon JL, Levens N (2002) Acute and chronic administration of melanin-concentrating hormone enhances food intake and body weight in Wistar and Sprague-Dawley rats. International journal of obesity and related metabolic disorders: journal of the International Association for the Study of Obesity 26:1289–1295

24. Devera A, Pascovich C, Lagos P, Falconi A, Sampogna S, Chase MH, Torterolo P (2015) Melanin-concentrating hormone (MCH) modulates the activity of dorsal raphe neurons. Brain Res 1598:114–128 [PubMed: 25541366]

25. Dilsiz P, Aklan I, Sayar Atasoy N, Yavuz Y, Filiz G, Koksalar F, Ates T, Oncul M, Coban I, Ates Oz E et al. (2020) MCH neuron activity is sufficient for reward and reinforces feeding. Neuroendocrinol 110:258–270

26. Diniz GB, Battagello DS, Klein MO, Bono BSM, Ferreira JGP, Motta-Teixeira LC, Duarte JCG, Presse F, Nahon JL, Adamantidis A et al. (2020) Ciliary melanin-concentrating hormone receptor 1 (MCHR1) is widely distributed in the murine CNS in a sex-independent manner. J Neurosci Res 98:2045–2071 [PubMed: 32530066]

27. Domire JS, Green JA, Lee KG, Johnson AD, Askwith CC, Mykytyn K (2011) Dopamine receptor 1 localizes to neuronal cilia in a dynamic process that requires the Bardet-Biedl syndrome proteins. Cell Mole life Scis: CMLS 68:2951–2960

28. Engle SE, Bansal R, Antonellis PJ, Berbari NF (2021) Cilia signaling and obesity. Semin Cell Dev Biol 110:43–50 [PubMed: 32466971]

29. Paxinos G, K.F. (2001). The mouse brain in stereotaxic coordinates. (Academic Press).

30. Garcia-Fuster MJ, Parks GS, Clinton SM, Watson SJ, Akil H, Civelli O (2012) The melanin-concentrating hormone (MCH) system in an animal model of depression-like behavior. Eur Neuropsychopharmacology: the journal of the European College of Neuropsychopharmacology 22:607–613

31. Gehlert DR, Rasmussen K, Shaw J, Li X, Ardayfio P, Craft L, Coskun T, Zhang HY, Chen Y, Witkin JM (2009) Preclinical evaluation of melanin-concentrating hormone receptor 1 antagonism for the treatment of obesity and depression. J Pharmacol Exp Ther 329:429–438 [PubMed: 19182070]

32. Gomori A, Ishihara A, Ito M, Mashiko S, Matsushita H, Yumoto M, Ito M, Tanaka T, Tokita S, Moriya M et al. (2003) Chronic intracerebroventricular infusion of MCH causes obesity in mice. Melanin-concentrating hormone. American journal of physiology. Endocrinol Metab 284:E583–588

33. Gonzalez JA, Iordanidou P, Strom M, Adamantidis A, Burdakov D (2016) Awake dynamics and brain-wide direct inputs of hypothalamic MCH and orexin networks. Nat Commun 7:11395 [PubMed: 27102565]
34. Gonzalez MI, Baker BI, Wilson CA (1997) Stimulatory effect of melanin-concentrating hormone on luteinising hormone release. Neuroendocrinology 66:254–262 [PubMed: 9349659]
35. Gonzalez MI, Vaziri S, Wilson CA (1996) Behavioral effects of alpha-MSH and MCH after central administration in the female rat. Peptides 17:171–177 [PubMed: 8822527]
36. Hamamoto A, Yamato S, Katoh Y, Nakayama K, Yoshimura K, Takeda S, Kobayashi Y, Saito Y (2016) Modulation of primary cilia length by melanin-concentrating hormone receptor 1. Cell Signal 28:572–584 [PubMed: 26946173]
37. Handel M, Schulz S, Stanarius A, Schreff M, Erdtmann-Vourliotis M, Schmidt H, Wolf G, Hollt V (1999) Selective targeting of somatostatin receptor 3 to neuronal cilia. Neuroscience 89:909–926 [PubMed: 10199624]
38. Hartwig C, Monis WJ, Chen X, Dickman DK, Pazour GJ, Faundez V (2018) Neurodevelopmental disease mechanisms, primary cilia, and endosomes converge on the BLOC-1 and BORC complexes. Dev Neurobiol 78:311–330 [PubMed: 28986965]
39. Hassani OK, Lee MG, Jones BE (2009) Melanin-concentrating hormone neurons discharge in a reciprocal manner to orexin neurons across the sleep-wake cycle. Proc Natl Acad Sci U S A 106:2418–2422 [PubMed: 19188611]
40. Hervieu GJ, Cluderay JE, Harrison D, Meakin J, Maycox P, Nasir S, Leslie RA (2000) The distribution of the mRNA and protein products of the melanin-concentrating hormone (MCH) receptor gene, slc-1, in the central nervous system of the rat. Eur J Neurosci 12:1194–1216 [PubMed: 10762350]
41. Hu L, Wang B, Zhang Y (2017) Serotonin 5-HT6 receptors affect cognition in a mouse model of Alzheimer's disease by regulating cilia function. Alzheimer's Res Ther 9:76 [PubMed: 28931427]
42. Humphries S (2013) A physical explanation of the temperature dependence of physiological processes mediated by cilia and flagella. Proc Natl Acad Sci USA 110:14693–14698 [PubMed: 23959901]
43. Kobayashi Y, Okada T, Miki D, Sekino Y, Koganezawa N, Shirao T, Diniz GB, Saito Y (2021) Properties of primary cilia in melanin-concentrating hormone receptor 1-bearing hippocampal neurons in vivo and in vitro. Neurochemistry international 142:104902 [PubMed: 33197527]
44. Kobayashi Y, Tomoshige S, Imakado K, Sekino Y, Koganezawa N, Shirao T, Diniz GB, Miyamoto T, and Saito Y Ciliary GPCR-based transcriptome as a key regulator of cilia length control. FASEB BioAdvances *n/a*.
45. Kong D, Vong L, Parton LE, Ye C, Tong Q, Hu X, Choi B, Bruning JC, Lowell BB (2010) Glucose stimulation of hypothalamic MCH neurons involves K(ATP) channels, is modulated by UCP2, and regulates peripheral glucose homeostasis. Cell Metab 12:545–552 [PubMed: 21035764]
46. Krashes MJ, Koda S, Ye C, Rogan SC, Adams AC, Cusher DS, Maratos-Flier E, Roth BL, Lowell BB (2011) Rapid, reversible activation of AgRP neurons drives feeding behavior in mice. J Clin Invest 121:1424–1428 [PubMed: 21364278]
47. Kuhara A, Okumura M, Kimata T, Tanizawa Y, Takano R, Kimura KD, Inada H, Matsumoto K, Mori I (2008) Temperature sensing by an olfactory neuron in a circuit controlling behavior of C. elegans. Sci 320:803–807
48. Lopez Hill X, Pascovich C, Urbanavicius J, Torterolo P, Scorza MC (2013) The median raphe nucleus participates in the depressive-like behavior induced by MCH: differences with the dorsal raphe nucleus. Peptides 50:96–99 [PubMed: 24126282]
49. Marsh DJ, Weingarth DT, Novi DE, Chen HY, Trumbauer ME, Chen AS, Guan XM, Jiang MM, Feng Y, Camacho RE et al. (2002) Melanin-concentrating hormone 1 receptor-deficient mice are lean, hyperactive, and hyperphagic and have altered metabolism. Proc Natl Acad Sci USA 99:3240–3245 [PubMed: 11867747]
50. Mattis J, Tye KM, Ferenczi EA, Ramakrishnan C, O'Shea DJ, Prakash R, Gunaydin LA, Hyun M, Fenno LE, Gradinaru V et al. (2011) Principles for applying optogenetic tools derived from direct comparative analysis of microbial opsins. Nat Methods 9:159–172 [PubMed: 22179551]

51. Miyoshi K, Kasahara K, Miyazaki I, Asanuma M (2009) Lithium treatment elongates primary cilia in the mouse brain and in cultured cells. Biochem Biophys Res Commun 388:757–762 [PubMed: 19703416]
52. Naganuma F, Bandaru SS, Absi G, Mahoney CE, Scammell TE, Vetrivelan R (2018) Melanin-concentrating hormone neurons contribute to dysregulation of rapid eye movement sleep in narcolepsy. Neurobiol Dis 120:12–20 [PubMed: 30149182]
53. Nahon JL, Presse F, Bittencourt JC, Sawchenko PE, Vale W (1989) The rat melanin-concentrating hormone messenger ribonucleic acid encodes multiple putative neuropeptides coexpressed in the dorsolateral hypothalamus. Endocrinology 125:2056–2065 [PubMed: 2477226]
54. Nauli SM, Jin X, AbouAlaiwi WA, El-Jouni W, Su X, Zhou J (2013) Non-motile primary cilia as fluid shear stress mechanosensors. Methods Enzymol 525:1–20 [PubMed: 23522462]
55. Noble EE, Hahn JD, Konanur VR, Hsu TM, Page SJ, Cortella AM, Liu CM, Song MY, Suarez AN, Szujewski CC et al. (2018) Control of feeding behavior by cerebral ventricular volume transmission of melanin concentrating hormone. Cell metabolism 28(55):68–e57
56. Nonaka S, Tanaka Y, Okada Y, Takeda S, Harada A, Kanai Y, Kido M, Hirokawa N (1998) Randomization of left-right asymmetry due to loss of nodal cilia generating leftward flow of extraembryonic fluid in mice lacking KIF3B motor protein. Cell 95:829–837 [PubMed: 9865700]
57. O'Callaghan C, Achaval M, Forsythe I, Barry PW (1995) Brain and respiratory cilia: the effect of temperature. Biol Neonate 68:394–397 [PubMed: 8721882]
58. Oh ST, Liu QF, Jeong HJ, Lee S, Samidurai M, Jo J, Pak SC, Park HJ, Kim J, Jeon S (2019) Nasal cavity administration of melanin-concentrating hormone improves memory impairment in memory-impaired and Alzheimer's disease mouse models. Mol Neurobiol 56:8076–8086 [PubMed: 31183806]
59. Omori Y, Chaya T, Yoshida S, Irie S, Tsujii T, Furukawa T (2015) Identification of G protein-coupled receptors GPCRs in primary cilia and their possible involvement in body weight control. PloS one 10:e0128422 [PubMed: 26053317]
60. Onaka T, Takayanagi Y, Yoshida M (2012) Roles of oxytocin neurones in the control of stress, energy metabolism, and social behaviour. J Neuroendocrinol 24:587–598 [PubMed: 22353547]
61. Parkes D, Vale W (1992) Secretion of melanin-concentrating hormone and neuropeptide-EI from cultured rat hypothalamic cells. Endocrinology 131:1826–1831 [PubMed: 1327720]
62. Paxinos GW, Charles. (2007). The rat brain in stereotaxic coordinates.
63. Pedersen CA, Caldwell JD, Walker C, Ayers G, Mason GA (1994) Oxytocin activates the postpartum onset of rat maternal behavior in the ventral tegmental and medial preoptic areas. Behav Neurosci 108:1163–1171 [PubMed: 7893408]
64. Pedersen CA, Prange AJ Jr (1979) Induction of maternal behavior in virgin rats after intracerebroventricular administration of oxytocin. Proc Natl Acad Sci USA 76:6661–6665 [PubMed: 293752]
65. Phan J, Alhassen L, Argelagos A, Alhassen W, Vachirakorntong B, Lin ZT, Sanathara N, and Alachkar A (2020). Mating and parenting experiences sculpture mood-modulating effects of oxytocin-MCH signaling. Sci Rep-Uk 10.
66. Reiter JF, Leroux MR (2017) Genes and molecular pathways underpinning ciliopathies. Nat Rev Mol Cell Biol 18:533–547 [PubMed: 28698599]
67. Rondini TA, Donato J Jr, Rodrigues Bde C, Bittencourt JC, Elias CF (2010) Chemical identity and connections of medial preoptic area neurons expressing melanin-concentrating hormone during lactation. J Chem Neuroanat 39:51–62 [PubMed: 19913090]
68. Saito Y, Cheng M, Leslie FM, Civelli O (2001) Expression of the melanin-concentrating hormone (MCH) receptor mRNA in the rat brain. J Comp Neurol 435:26–40 [PubMed: 11370009]
69. Saito Y, Nothacker HP, Wang Z, Lin SH, Leslie F, Civelli O (1999) Molecular characterization of the melanin-concentratinghormone receptor. Nature 400:265–269 [PubMed: 10421368]
70. Sanathara NM, Garau C, Alachkar A, Wang L, Wang Z, Nishimori K, Xu X, Civelli O (2018) Melanin concentrating hormone modulates oxytocin-mediated marble burying. Neuropharmacology 128:22–32 [PubMed: 28888943]
71. Schneider CA, Rasband WS, Eliceiri KW (2012) NIH image to ImageJ: 25 years of image analysis. Nat Methods 9:671–675 [PubMed: 22930834]

72. Shearman LP, Camacho RE, Sloan Stribling D, Zhou D, Bednarek MA, Hreniuk DL, Feighner SD, Tan CP, Howard AD, Van der Ploeg LH et al. (2003) Chronic MCH-1 receptor modulation alters appetite, body weight and adiposity in rats. Eur J Pharmacol 475:37–47 [PubMed: 12954357]
73. Shimazaki T, Yoshimizu T, Chaki S (2006) Melanin-concentrating hormone MCH1 receptor antagonists: a potential new approach to the treatment of depression and anxiety disorders. CNS Drugs 20:801–811 [PubMed: 16999451]
74. Stanic D, Malmgren H, He H, Scott L, Aperia A, Hokfelt T (2009) Developmental changes in frequency of the ciliary somatostatin receptor 3 protein. Brain Res 1249:101–112 [PubMed: 18992731]
75. Tomoshige S, Kobayashi Y, Hosoba K, Hamamoto A, Miyamoto T, Saito Y (2017) Cytoskeleton-related regulation of primary cilia shortening mediated by melanin-concentrating hormone receptor 1. Gen Comp Endocrinol 253:44–52 [PubMed: 28842217]
76. Torterolo P, Lagos P, Sampogna S, Chase MH (2008) Melanin-concentrating hormone (MCH) immunoreactivity in non-neuronal cells within the raphe nuclei and subventricular region of the brainstem of the cat. Brain Res 1210:163–178 [PubMed: 18410908]
77. Tsang SH, Aycinena ARP, Sharma T (2018) Ciliopathy: Bardet-Biedl syndrome. Adv Exp Med Biol 1085:171–174 [PubMed: 30578506]
78. Urbanavicius J, Lagos P, Torterolo P, Abin-Carriquiry JA, Scorza C (2016) Melanin-concentrating hormone projections to the dorsal raphe nucleus: an immunofluorescence and in vivo microdialysis study. J Chem Neuroanat 72:16–24 [PubMed: 26686290]
79. Urbanavicius J, Lagos P, Torterolo P, Scorza C (2014) Prodepressive effect induced by microinjections of MCH into the dorsal raphe: time course, dose dependence, effects on anxiety-related behaviors, and reversion by nortriptyline. Behav Pharmacol 25:316–324 [PubMed: 25006977]
80. Valente EM, Rosti RO, Gibbs E, Gleeson JG (2014) Primary cilia in neurodevelopmental disorders. Nat Rev Neurol 10:27–36 [PubMed: 24296655]
81. Varela L, Horvath TL (2018) Neuronal cilia: another player in the melanocortin system. Trends Mol Med 24:333–334 [PubMed: 29501261]
82. Vawter MP, Schulmann A, Alhassen L, Alhassen W, Hamzeh AR, Sakr J, Pauluk L, Yoshimura R, Wang X, Dai Q, et al. (2019). Melanin concentrating hormone signaling deficits in schizophrenia: association with memory and social impairments and abnormal sensorimotor gating. The international journal of neuropsychopharmacology.
83. Vawter MP, Schulmann A, Alhassen L, Alhassen W, Hamzeh AR, Sakr J, Pauluk L, Yoshimura R, Wang X, Dai Q et al. (2020) Melanin concentrating hormone signaling deficits in schizophrenia: association with memory and social impairments and abnormal sensorimotor gating. Int J Neuropsychopharmacol 23:53–65 [PubMed: 31563948]
84. Vawter MP, Schulmann A, Alhassen L, Alhassen W, Hamzeh AR, Sakr J, Pauluk L, Yoshimura R, Wang X, Dai Q et al. (2020) Melanin concentrating hormone signaling deficits in schizophrenia: association with memory and social impairments and abnormal sensorimotor gating. Int J Neuropsychoph 23:53–65
85. Wheatley DN (2008) Nanobiology of the primary cilium–paradigm of a multifunctional nanomachine complex. Methods Cell Biol 90:139–156 [PubMed: 19195549]
86. Yoshiba S, Shiratori H, Kuo IY, Kawasumi A, Shinohara K, Nonaka S, Asai Y, Sasaki G, Belo JA, Sasaki H et al. (2012) Cilia at the node of mouse embryos sense fluid flow for left-right determination via Pkd2. Science 338:226–231 [PubMed: 22983710]
87. Zhang Q, Nishimura D, Seo S, Vogel T, Morgan DA, Searby C, Bugge K, Stone EM, Rahmouni K, Sheffield VC (2011) Bardet-Biedl syndrome 3 (Bbs3) knockout mouse model reveals common BBS-associated phenotypes and Bbs3 unique phenotypes. Proc Natl Acad Sci USA 108:20678–20683 [PubMed: 22139371]

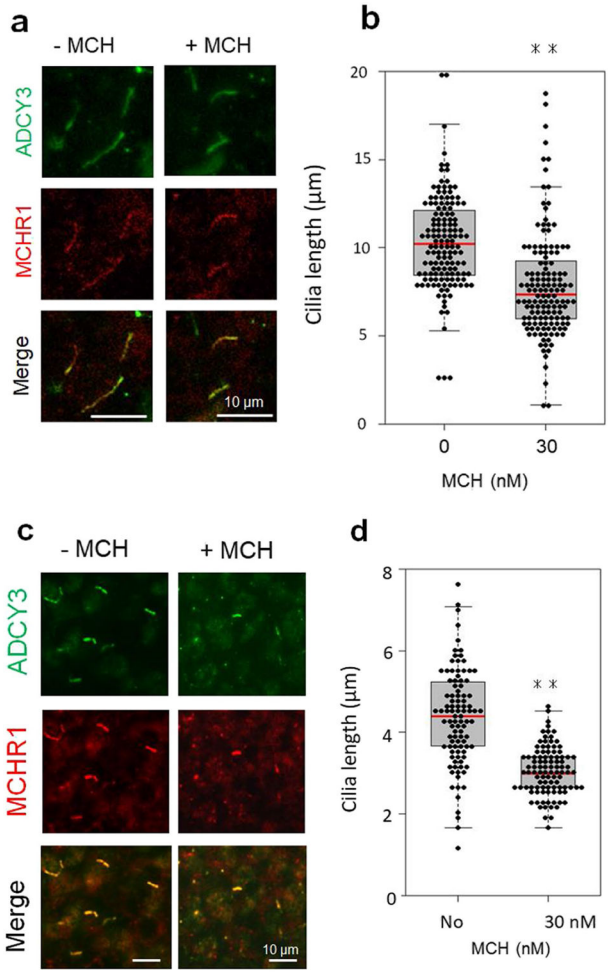

Fig. 1.

MCH treatment leads to cilia length shortening in cultured brain slices. CPu and PFC slices were treated with MCH on days 14 or 7 of culture, respectively. **a, b** Rat CPu slice cultures were treated with vehicle or 30 nM MCH for 18 h. **c, d** Rat PFC slice cultures were treated with vehicle or 30 nM MCH for 6 h. **a, c** Primary cilia were co-labeled with antibodies against ADCY3 (green) and MCHR1 (red). Scale bars = 10 µm. **b, d** The scatter plot represents cilium lengths measured using ADCY3/MCHR1 double labeling in randomly selected fields; at least 80 cilia per group in both CPu slices (**b**) and PFC slices (**d**) were evaluated, respectively. Primary cilia were significantly shorter in MCH-treated cultures than in control cultures for both CPu slices and PFC slices. Unpaired *t* test, $^{**}P < 0.01$. Data are presented as means ± SEM

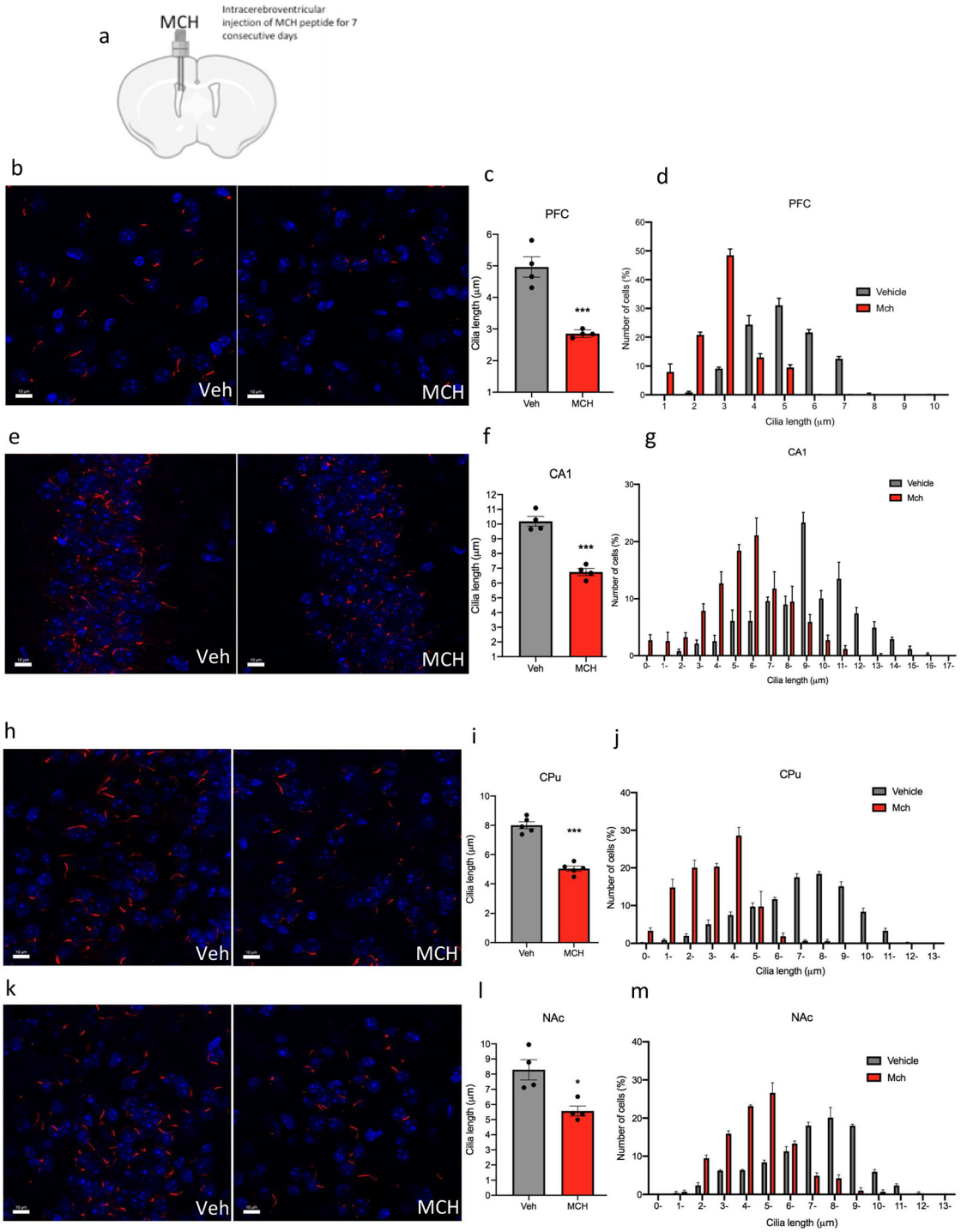

Fig. 2.

Chronic intracerebroventricular administration of MCH to mice shortens cilia length. **a** Schematic representation of chronic intracerebroventricular administration of MCH peptide. Male mice were administered with vehicle or MCH (1 nmol). Diagram was created with BioRender.com webpage. **b, e, h, k** Immunostaining of ADCY3 labeled in red fluorescence and counterstained with DAPI (blue) in the **b** PFC, **e** CA1, **h** CPu, and **k** NAc in animals

administered with MCH or vehicle (scale bar = 10 μm, magnification = 63 ×). **c, e, g, i** Quantification of the length of ADCY3 + primary cilia (μm) in the **c** PFC, **e** CA1, **g** CPu, and (**i**) NAc in animals administered with MCH or vehicle, ***$P < 0.0007$ and **$P < 0.01$. **d, g, j, m** Cilia were grouped by length (μm) and plotted against the number of cells (%) in the **d** PFC, **g** CA1, **j** CPu, and **m** NAc

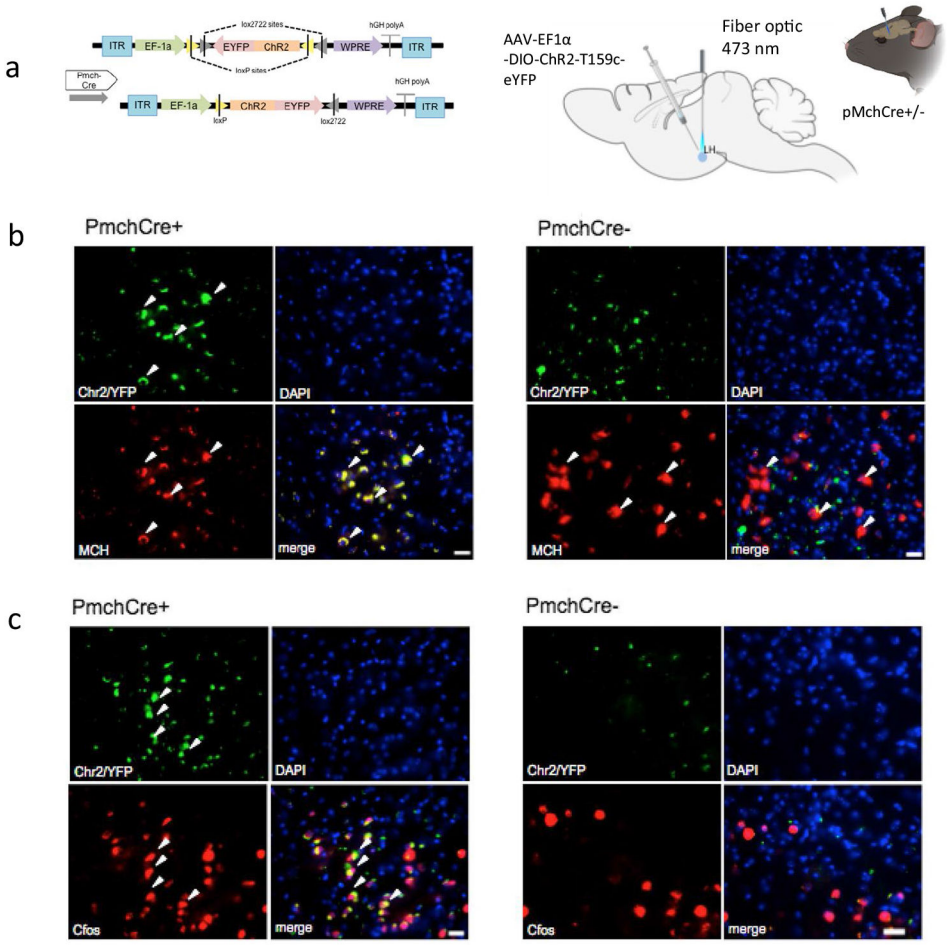

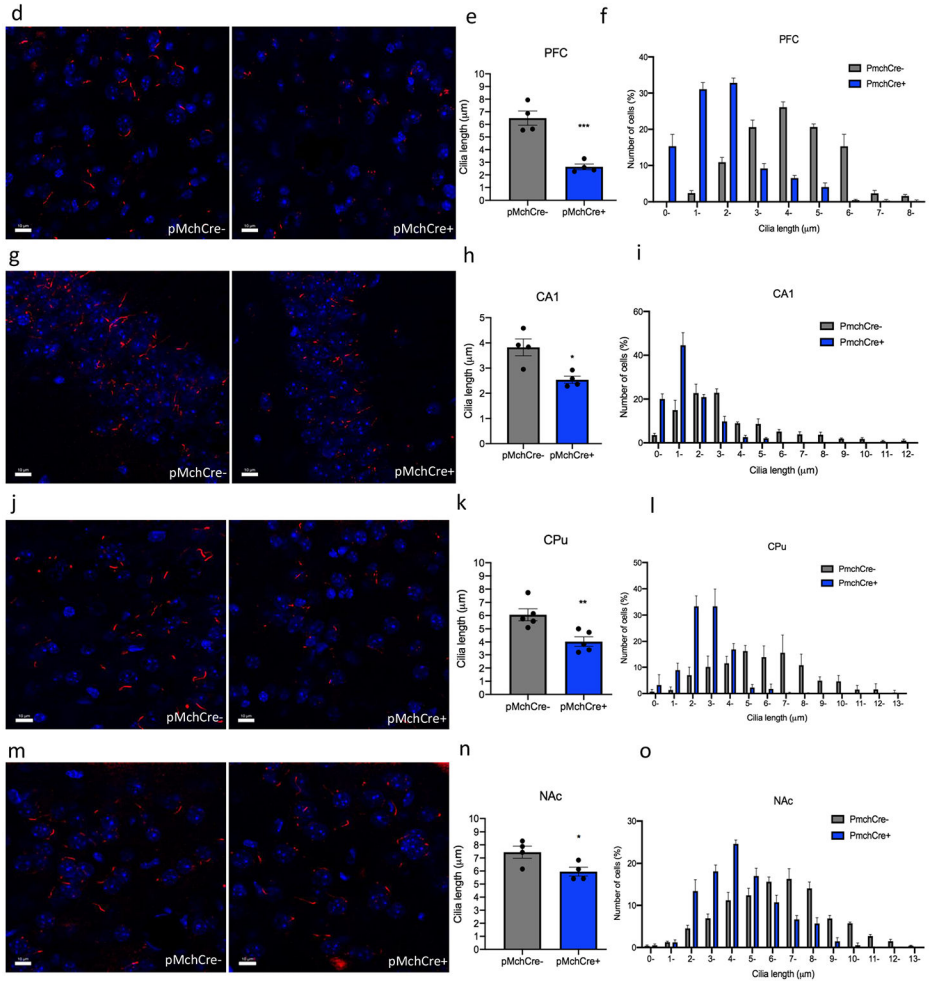

Fig. 3.

Optogenetic stimulation of MCH shortens cilia length. **a** Experimental approach. Adult PmchCre + and PmchCre− mice were stereotaxically injected with AAV-EF1α-DIO-ChR2-T159c-eYFP in the lateral hypothalamus (LH). A fiber cannula was then placed in the LH slightly above the injection site. Diagram was created with BioRender.com webpage. **b** Coexpression of ChR2 (green) containing neurons in the lateral hypothalamus and MCH immunofluorescence (red) and counterstained with DAPI (blue) in PmchCre + and PmchCre− mice. (scale bar = 10 µm, magnification = 40×). **c** ChR2 fluorescence (green) and c-Fos immunofluorescence (red) identifies cells recently activated in PmchCre + and PmchCre− mice (scale bar = 10 µm). **d, g, j, m** Immunostaining of ADCY3 labeled in red fluorescence in the **d** PFC, **g** CA1, **j** CPu, and **m** NAc after blue light activation in PmchCre + and PmchCre− mice (scale bar = 10 µm). **e, h, k, n** Quantification of the length of ADCY3 + primary cilia (µm) in the **e** PFC, **h** CA1, **k** CPu, and **n** NAc, $*P < 0.05$, $**P < 0.01$, and $***P < 0.001$. **f, I, l, o** Cilia were grouped by length (µm) and plotted against the number of cells (%) in the **f** PFC, **i** CA1, **l** CPu, and **o** NAc

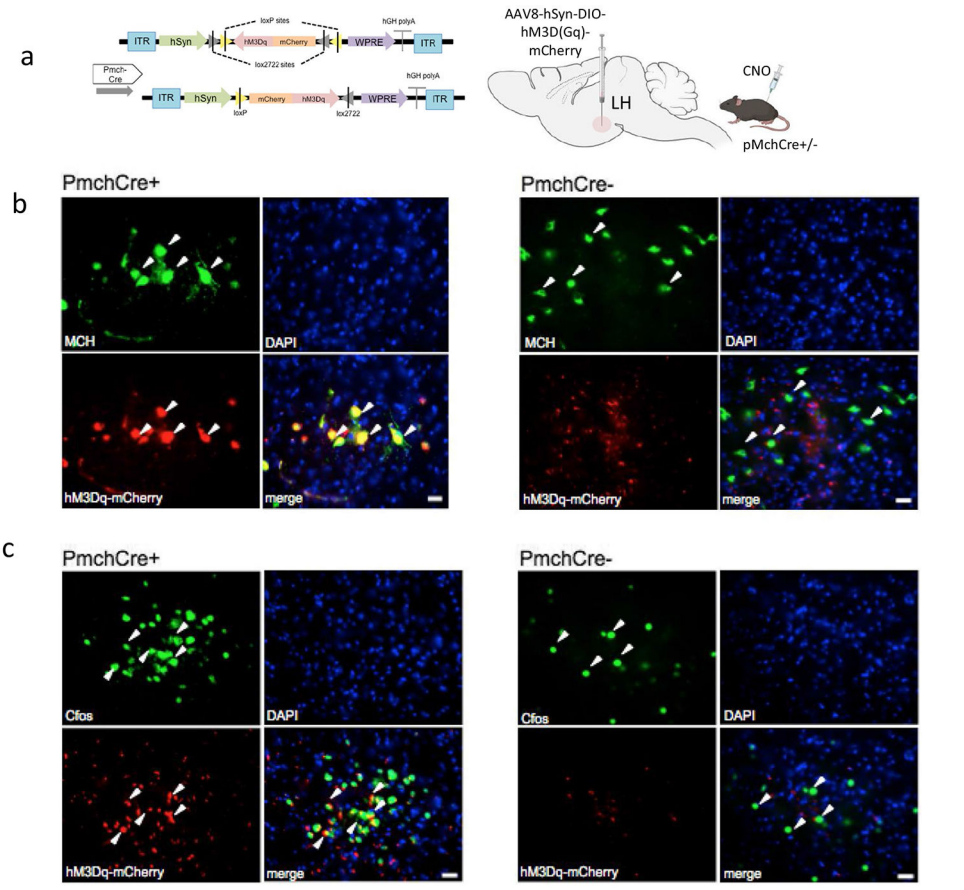

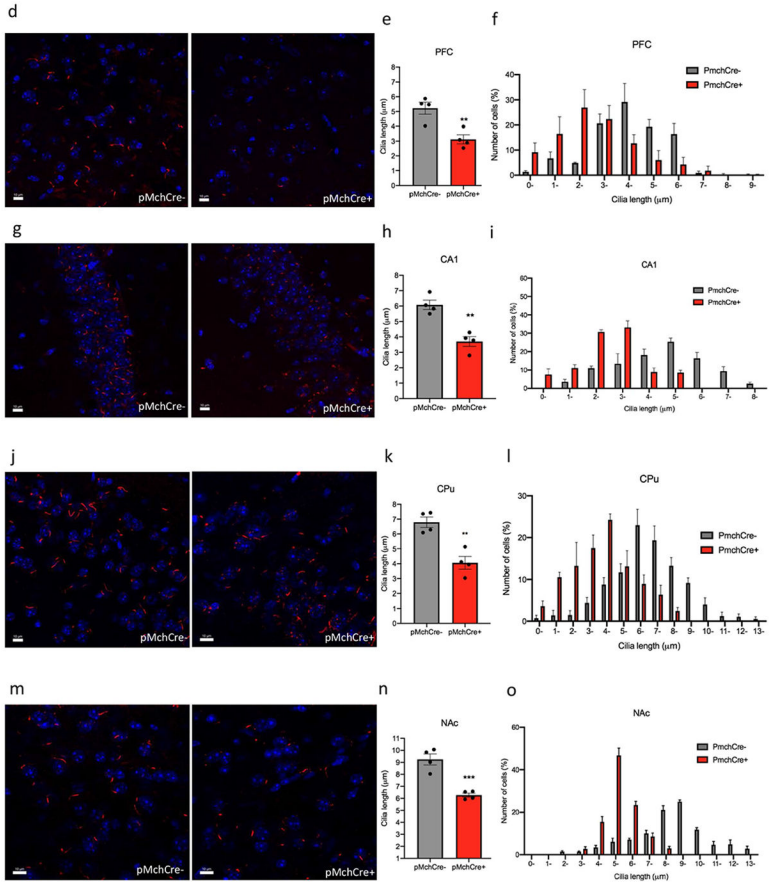

Fig. 4.

Chemogenic excitation of MCH shortens cilia length. **a** Experimental approach. Adult PmchCre + and PmchCre− mice underwent bilateral stereotaxic injection in the lateral hypothalamus with AAV-hSyn-DIO-hM3D(Gq)-mCherry to express DREADD in Cre-expressing MCH neurons. Clozapine-N-oxide (CNO) was delivered intraperitoneally to stimulate MCH neurons. Diagram was created with BioRender.com webpage. **b** Co-expression of mCherry fluorescence (red) identifying DREADD-expressing neurons and MCH immunofluorescence (green) and counterstained with DAPI (blue) in Pmch-Cre+and PmchCre− mice (scale bar = 10 µm, magnification = 40 ×). **c** mCherry fluorescence (red) identifies DREADD-expressing neurons, and c-Fos immunofluorescence (green) identifies cells recently activated in PmchCre + and PmchCre− mice (Scale bar = 10 µm). **d, g, j, m** Immunostaining of ADCY3 labeled in red fluorescence in the **d** PFC, **g** CA1, **j** CPu and **m** NAc via CNO-dependent activation of Gq signaling in PmchCre + and PmchCre− mice (scale bar = 10 µM). **e, h, k, n**) Quantification of the length of ADCY3 + primary cilia in the **e** PFC, **h** CA1, **k** CPu, and **n** NAc, $^{**}P < 0.01$ and $^{***}P < 0.001$. **f, i, l, o** Cilia were grouped by length (µm) and plotted against the number of cells (%) in the **f** PFC, **i** CA1, **l** CPu, and **o** NAc

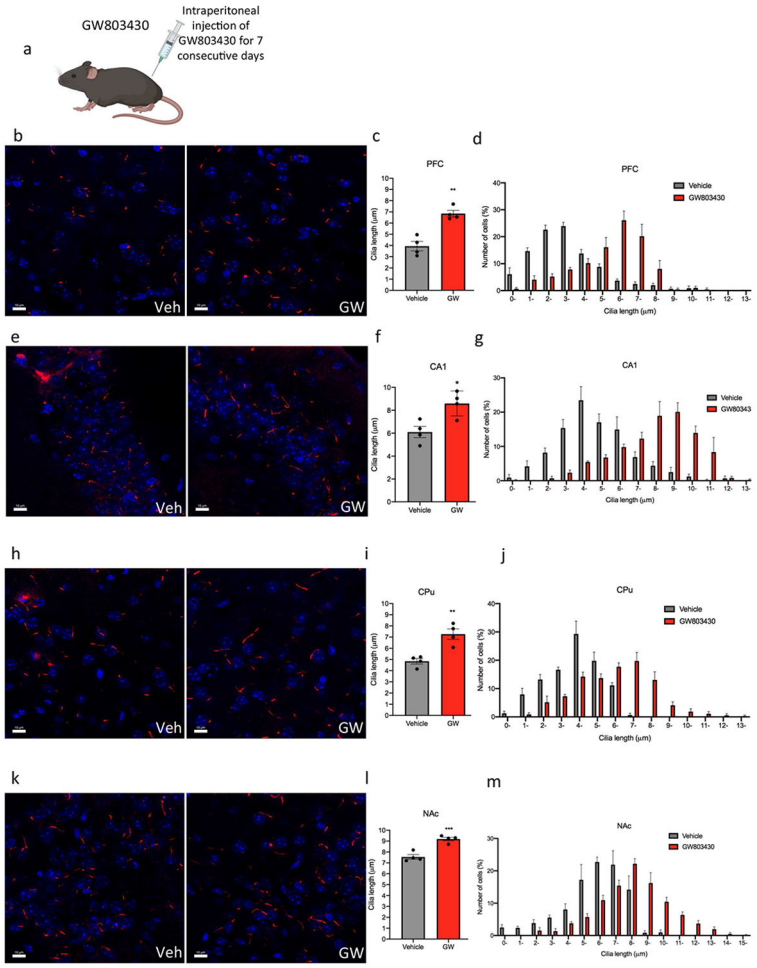

Fig. 5.

Systemic administration of the GW803430 (MCHR1 antagonist) to mice increases cilia length. **a** Schematic representation of systemic administration of GW803430 or vehicle for 7 consecutive days in adult mice. Diagram was created with BioRender.com webpage. **b, e, h, k** Immunostaining of ADCY3 labeled in red fluorescence in the **b** PFC, **e** CA1, **h** CPu, and **k** NAc in animals administered with GW803430 or vehicle (scale bar = 10 µm). **c, f, I, l** Quantification of the length of ADCY3 + primary cilia in the **c** PFC, **f** CA1, **i** CPu, and **l** NAc in animals administered with GW803430 or vehicle, $*P < 0.05$, $**P < 0.01$, and $***P < 0.001$. **d, g, j, m** Cilia were grouped by length (µm) and plotted against the number of cells (%) in the **d** PFC, **g** CA1, **j** CPu, and **m** NAc

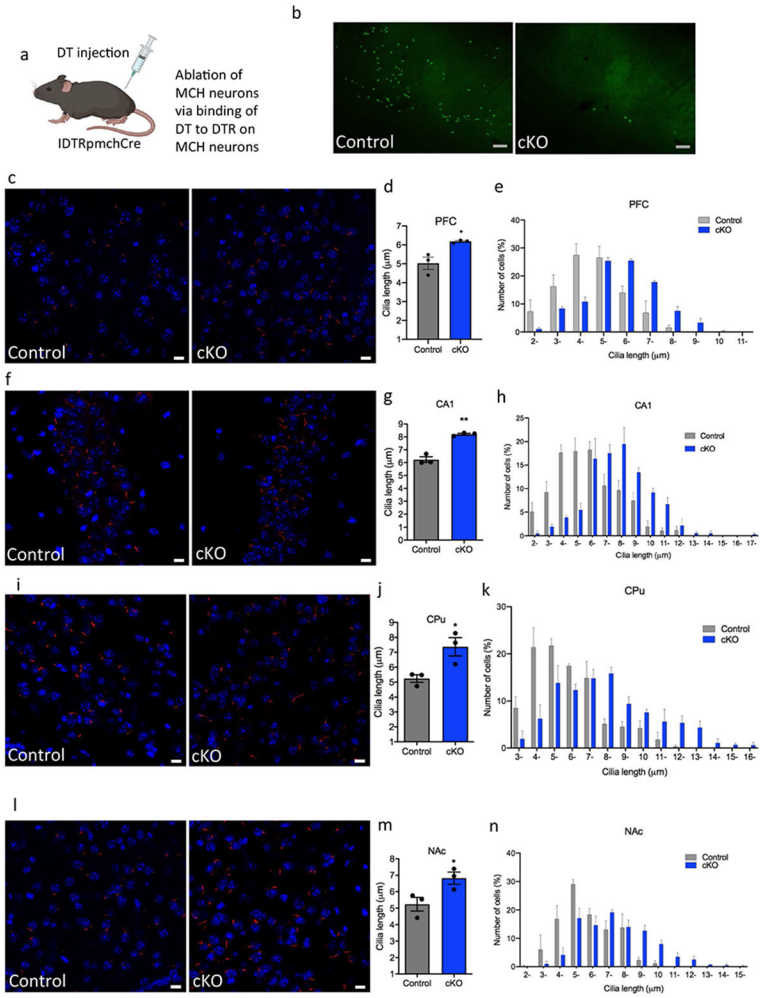

Fig. 6.

Cilia length is increased in MCH deficit mice. **a** Schematic representation of how the MCH cells are ablated through DTR. IDTR mice were crossed with PmchCre mice rendering offspring mice with Cre-expressing MCH neurons sensitive to DT. Diagram was created with BioRender.com webpage. **b** MCH immunoreactivity (GFP) in the lateral hypothalamus of IDTRPmchCre− and IDTRPmchCre + mice following DT injection (scale bar = 100 µm, magnification = 10 ×). **c, f, I, l** Immunostaining of ADCY3 labeled in red fluorescence and counterstained with DAPI (blue) in IDTRPmch + and IDTRPmch− mice in the **c** PFC, **e** CA1, **g** CPu, and **i** NAc (scale bar = 10 µm, magnification = 63 ×). **d, g, j, m** Quantification of cilia length (µm) in the **d** PFC, **f** CA1, **h** CPu, and **j** NAc, $*P < 0.05$ and $**P < 0.01$. **e, h, k, n** Cilia were grouped by length (µm) and plotted against the number of cells (%) in the **e** PFC, **h** CA1, **k** CPu, and **n** NAc

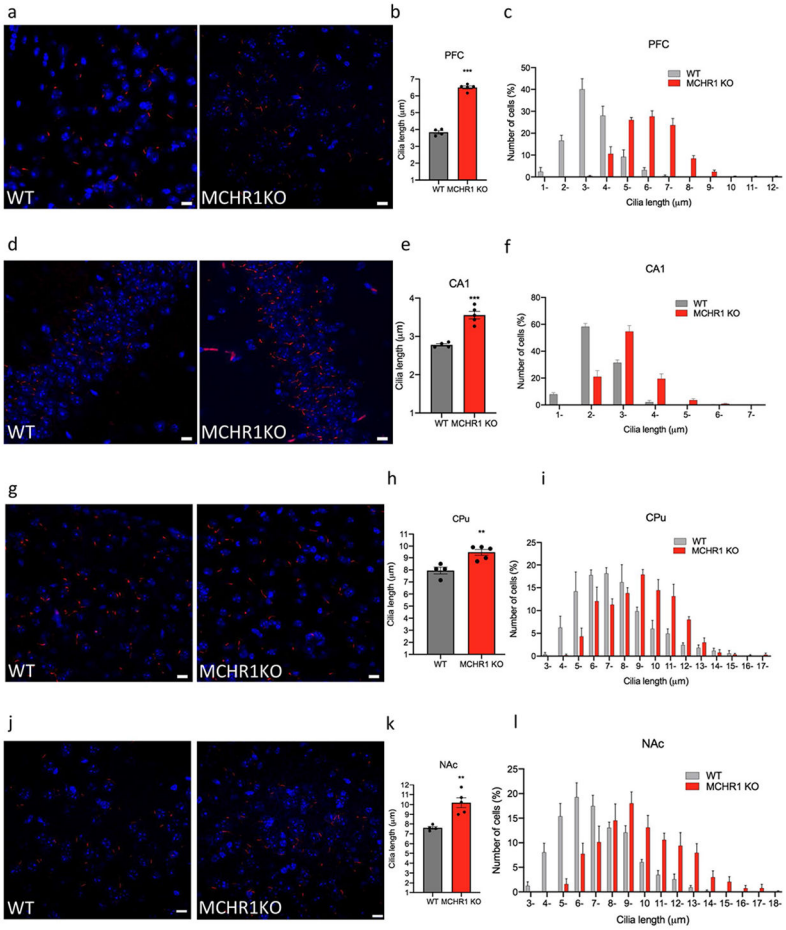

Fig. 7.

Cilia length is increased in MCHR1 knockout animals. Immunostaining of ADCY3 labeled in red fluorescence and counterstained with DAPI (blue) in the **a** PFC, **d** CA1, **g** CPu, and **j** NAc in MCHR1 KO or WT mice (scale bar = 10 µm, magnification = 63 ×. **b, e, h, k** Quantification of the length of ADCY3^{+} primary cilia (µm) in the **b** PFC, **e** CA1, **h** CPu (CPu), and **k** NAc in MCHR1 KO or WT mice, $^{**}P < 0.01$ and $^{***}P < 0.001$. **c, f, I, l** Cilia were grouped by length (µm) and plotted against the number of cells (%) in the **c** PFC, **f** CA1, **i** CPu, and **l** NAc

Table 1

Mouse genetic background and routes of drug/virus administrations

Experiment	Genetic background	Route of administration	Vendor
MCH	Swiss Webster	Intracerebroventricular injection	Charles River
GW803430	Swiss Webster	Intraperitoneal injection	Charles River
Optogenetics pMCHCre	C57BL/6	Stereotaxic injection of AAV	Tg(pMCH-cre)1Lowl/J mice, Jackson Laboratories
Chemogenics pMCHCre	C57BL/6	Stereotaxic injection of AAV, and intraperitoneal injection of CNO	Tg(pMCH-cre)1Lowl/J mice, Jackson Laboratories
IDTR pMCHCre	C57BL/6	Intraperitoneal injection of DT	Tg(pMCH-cre)1Lowl/J mice, Jackson Laboratories
MCHR1 KO	BL6-Taconic	N/A	Dr. Su Qian (Merck, Rahway, NJ)